JAERI - M
88-092

ICRF ENHANCEMENT OF FUSION REACTIVITY IN THE PRESENCE OF ALPHA PARTICLES

May 1988

Mitsuru YAMAGIWA and Tomonori TAKIZUKA

日 本 原 子 力 研 究 所
Japan Atomic Energy Research Institute

JAERI-Mレポートは，日本原子力研究所が不定期に公刊している研究報告書です。
入手の問合わせは，日本原子力研究所技術情報部情報資料課（〒319-11茨城県那珂郡東海村）あて，お申しこしください。なお，このほかに財団法人原子力弘済会資料センター（〒319-11 茨城県那珂郡東海村日本原子力研究所内）で複写による実費頒布をおこなっております。

JAERI-M reports are issued irregularly.
Inquiries about availability of the reports should be addressed to Information Division, Department of Technical Information, Japan Atomic Energy Research Institute, Tokai-mura, Naka-gun, Ibaraki-ken 319-11, Japan.

編集兼発行　日本原子力研究所
印　　刷　㈱原子力資料サービス

JAERI-M 88-092

ICRF Enhancement of Fusion Reactivity in the Presence of Alpha Particles

Mitsuru YAMAGIWA and Tomonori TAKIZUKA

Department of Thermonuclear Fusion Research
Naka Fusion Research Establishment
Japan Atomic Energy Research Institute
Naka-machi, Naka-gun, Ibaraki-ken

(Received April 21, 1988)

Absorption of ICRF (ion cyclotron range of frequency) waves by alpha particles and fusion reactivity enhancement due to the ICRF induced ion tail are investigated. The rate of linear absorption by alpha particles increases with the cyclotron harmonic number, and decreases with the ratio of the electron plasma frequency to the electron cyclotron frequency. The deformation of the distribution due to ICRF waves is also examined by using a solution to a Fokker-Planck equation combined with a quasi-linear RF (radiofrequency) diffusion term. It is found that second harmonic ICRF heating is comparatively applicable to the enhancement of the fusion power density even in the presence of alpha particles, while the efficiency of the enhancement is deteriorated markedly by wave deposition to alphas for higher harmonic ICRF heating in the high magnetic field.

Keywords: Alpha Particle, ICRF Heating, Fusion Reactivity, Burn Control, D-T Plasma, Fokker-Planck Equation, Quasi-Linear RF Diffusion

JAERI－M 88－092

アルファ粒子の存在下におけるＩＣＲＦ波による核融合反応特性の向上

日本原子力研究所那珂研究所核融合研究部
山極　　満・滝塚　知典

（1988年４月21日受理）

アルファ粒子によるＩＣＲＦ（イオンサイクロトロン周波数帯）波の吸収およびＩＣＲＦ誘起イオンテイルによる核融合反応特性の向上について研究する。アルファ粒子による線型吸収率はサイクロトロン高調波の次数とともに増大し，電子サイクロトロン周波数に対するプラズマ周波数の比とともに減少する。準線型ＲＦ（高周波）拡散項を含むフォッカープランク方程式の解を用いて，ＩＣＲＦ波による分布関数の変形も解析する。第２高調波ＩＣＲＦ加熱はアルファ粒子の存在下においても核融合パワー密度を向上させるのに比較的適している。しかるに，強磁場中におけるより高い次数の高調波ＩＣＲＦ加熱に対しては，アルファ粒子による波の吸収が向上率を著しく悪化させることが見い出される。

那珂研究所：〒311－01　茨城県那珂郡那珂町大字向山801－1

Contents

目　　次

1. INTRODUCTION

Alpha particles produced by thermonuclear fusion reactions can interact with some radiofrequency (RF) waves. Wong and Ono showed that energetic alpha particles tend to absorb both the slow and fast waves in the lower hybrid frequency range, which can be a serious obstacle in fusion reactor current drive [1]. According to Bonoli and Porkolab [2], however, significant alpha particle damping of the slow wave may be avoided because of the combined effects of the wave propagation in the plasma outer region restricted by the conditions for wave accessibility and electron Landau damping and of the peaked nature of the alpha particle density profile near the plasma centre. Ion cyclotron range of frequency (ICRF) waves utilized to heat up D-T plasmas to the ignition temperature can be wasted by the produced alpha particles, since the alpha cyclotron frequency coincides with the deuteron cyclotron frequency. In addition, the RF induced anomalous diffusion of the alpha particles may lead to a reduction of the heating rate by them. On the other hand, if the alpha flux and the production rate of trapped alpha particles can be controlled by the RF waves, the alpha ash removal and the burn control may be possible. The fusion reactivity enhancement due to the ICRF induced ion tail [3-11] may also lead to the active burn control under the sub-ignition state. In the active burn control of nearly ignited plasmas, the fusion energy multiplication factor, Q, is the most crucial parameter. Then, it is important to study the effect of ICRF wave absorption by alpha particles on Q.

In this paper, ICRF enhancement of the fusion reactivity is investigated by taking into account of the wave absorption by alpha particles. The rate of ICRF absorption by alpha particles is studied not only for the slowing-down distribution but also for the distribution obtained by solving a Fokker-Planck quasi-linear equation [6,10-12]. Of particular interest is local power absorption by fuel ions and alpha particles in D-T plasmas; attention is paid to absorption of ICRF waves near the plasma centre, considering the centrally peaked nature of the alpha particle density profile. Therefore, spatial diffusion of the alpha particles is not taken into account. The ICRF heated particles are assumed to be diffused perpendicularly to the magnetic field in velocity space. In the velocity diffusion coefficient, the right circularly polarized amplitude of the RF electric

field as well as the left one is taken into account [10].

In Section 2 model equations are described. In Section 3 absorption of ICRF waves by alpha particles and ICRF enhancement of the fusion reactivity are studied. In Section 4 conclusions are presented.

2. MODEL EQUATIONS

The steady-state distribution function of i-species heated by the ICRF wave is assumed to be governed by

$$C(f_i) + Q(f_i) + S_i = 0 , \tag{1}$$

where $C(f_i)$ is the collision term, $Q(f_i)$ the quasi-linear RF diffusion term, and S_i the particle source term, respectively. As for $C(f_i)$, the linearized Fokker-Planck collision term is adopted. In the toroidal configuration, the width of the wave-particle resonance region in the direction of velocity parallel to the magnetic field is given by

$$\Delta v_{\parallel} = \frac{\omega}{k_{\parallel}} \frac{r_R}{R_0} , \tag{2}$$

where $\omega = N\,\omega_{ci}$ is the wave frequency, ω_{ci} the ion cyclotron frequency, N the cyclotron harmonic number, $k_{\parallel}$ the parallel wave number. The wave deposition region near the plasma centre on the minor cross section is specified, $r \leqq r_R$, and R_0 is the major radius of the torus. The comparatively small $k_{\parallel}$ is chosen such that the alpha birth speed, $v_0 = \sqrt{2E_\alpha/m_\alpha}$ (E_α is the alpha birth energy of 3.52 MeV and m_α is the mass of the alpha particle), is placed within $\Delta v_{\parallel}$ for finite but small r_R/R_0 and that the electron Landau damping of the wave is insignificant. The quasi-linear term, $Q(f_i)$, which describes the perpendicular heating of the particle due to the ICRF wave is given by

$$Q(f_i) = \frac{1}{v_\perp} \frac{\partial}{\partial v_\perp} \left(v_\perp D_{\perp i} \frac{\partial f_i}{\partial v_\perp} \right) , \tag{3}$$

where $v_\perp$ is the velocity component perpendicular to the magnetic field and

field as well as the left one is taken into account [10].

In Section 2 model equations are described. In Section 3 absorption of ICRF waves by alpha particles and ICRF enhancement of the fusion reactivity are studied. In Section 4 conclusions are presented.

2. MODEL EQUATIONS

The steady-state distribution function of i-species heated by the ICRF wave is assumed to be governed by

$$C(f_i) + Q(f_i) + S_i = 0 \ , \tag{1}$$

where $C(f_i)$ is the collision term, $Q(f_i)$ the quasi-linear RF diffusion term, and S_i the particle source term, respectively. As for $C(f_i)$, the linearized Fokker-Planck collision term is adopted. In the toroidal configuration, the width of the wave-particle resonance region in the direction of velocity parallel to the magnetic field is given by

$$\Delta v_{\parallel} = \frac{\omega}{k_{\parallel}} \frac{r_R}{R_0} \ , \tag{2}$$

where $\omega = N\ \omega_{ci}$ is the wave frequency, ω_{ci} the ion cyclotron frequency, N the cyclotron harmonic number, $k_{\parallel}$ the parallel wave number. The wave deposition region near the plasma centre on the minor cross section is specified, $r \leqq r_R$, and R_0 is the major radius of the torus. The comparatively small $k_{\parallel}$ is chosen such that the alpha birth speed, $v_0 = \sqrt{2E_\alpha/m_\alpha}$ (E_α is the alpha birth energy of 3.52 MeV and m_α is the mass of the alpha particle), is placed within $\Delta v_{\parallel}$ for finite but small r_R/R_0 and that the electron Landau damping of the wave is insignificant. The quasi-linear term, $Q(f_i)$, which describes the perpendicular heating of the particle due to the ICRF wave is given by

$$Q(f_i) = \frac{1}{v_\perp} \frac{\partial}{\partial v_\perp} \left(v_\perp\ D_{\perp i}\ \frac{\partial f_i}{\partial v_\perp} \right) \ , \tag{3}$$

where $v_\perp$ is the velocity component perpendicular to the magnetic field and

$D_{\perp i}$ the perpendicular diffusion coefficient due to the ICRF wave;

$$D_{\perp i} \propto \frac{1}{\omega} \frac{z_i^2 e^2}{m_i^2} |E_+|^2 \left\{ J_{N-1}^2\left(\frac{k_\perp v_\perp}{\omega_{ci}}\right) + \frac{|E_-|^2}{|E_+|^2} J_{N+1}^2\left(\frac{k_\perp v_\perp}{\omega_{ci}}\right) \right\} . \tag{4}$$

Here, z_i is the charge number, m_i the mass of i-species, e the elementary charge, J_l the Bessel function of the first kind of order l, $k_\perp$ the perpendicular wave number, $|E_+|$ and $|E_-|$ are the left and the right circularly polarized amplitudes of the RF electric field, respectively. When ω is chosen as an even harmonic resonance of ω_{cD}, $\omega = 2n\omega_{cD}$, all ion species, D, T, and α, interact with the RF wave. On the other hand, when $\omega = (2n+1)\omega_{cD}$, D and α can interact with the wave but tritons cannot, i.e., $D_{\perp T} = 0$. In the present calculation, the ratio of the polarization amplitudes, $|E_-|^2/|E_+|^2$, and $k_\perp$ are determined from the cold plasma dispersion relation [13];

$$\frac{|E_-|^2}{|E_+|^2} \simeq \left(\frac{K_\perp - K_\times}{K_\perp + K_\times} \right)^2 , \tag{5}$$

$$n^2_\perp = \frac{c^2 k_\perp^2}{\omega^2} \simeq K_\perp - \frac{K_\times^2}{K_\perp} , \tag{6}$$

where c is the speed of light, and $K_\perp$ and $K_\times$ are the well-known components of the cold plasma dielectric tensor ($K_\perp$ and $K_\times$ coincide with S and D in Ref.[14], respectively). The particle source terms for D and T are taken to be zero, and S_α which originates from fusion reactions is given by

$$S_\alpha = \frac{S_0}{4\pi v^2} \delta(v - v_0) \quad \text{with} \quad S_0 = n_D n_T \langle \sigma v \rangle , \tag{7}$$

where v is the particle speed, n_i the number density of i-species, and $\langle \sigma v \rangle$ the D-T fusion reactivity. The loss of alpha particles, which is restricted by the particle conservation, is assumed to occur in the very low energy region.

For the distribution isotropic in the pitch angle in velocity space, the deposited RF power density is given by

$$P_{RF,i} = \int d^3v \, \frac{1}{2} m_i v^2 \, Q(f_i)$$

$$= \int d^3v \, \frac{1}{2} m_i v^2 \, \frac{1}{v^2} \frac{d}{dv} \{ D_{\perp i} \, v^2 \, (1 - \xi^2) \, \frac{df_i}{dv} \}$$

$$\propto - 4 \pi m_i \, \frac{1}{\omega} \, \frac{z_i^2 e^2}{m_i^2} \, |E_+|^2 \int_0^\infty dv \, v^3 \, \frac{df_i}{dv} \int_0^1 d\xi \, (1 - \xi^2)$$

$$\times \left\{ J_{N-1}^2 \left(\frac{k_\perp v}{\omega_{ci}} \sqrt{1-\xi^2} \right) + \frac{|E_-|^2}{|E_+|^2} \, J_{N+1}^2 \left(\frac{k_\perp v}{\omega_{ci}} \sqrt{1-\xi^2} \right) \right\} , \qquad (8)$$

where ξ is the cosine of the pitch angle, θ ($\xi = \cos\theta$). The rate of absorption of the ICRF wave by i-species is defined by $R_i \equiv P_{RF,i} / P_{RF}$ with $P_{RF} = P_{RF,D} + P_{RF,T} + P_{RF,\alpha}$.

Linear absorption of ICRF waves is studied for the distributions;

$$f_D = \frac{n_D}{(2\pi T/m_D)^{3/2}} \exp \left(- \frac{m_D}{2T} v^2 \right) , \qquad (9a)$$

$$f_T = \frac{n_T}{(2\pi T/m_T)^{3/2}} \exp \left(- \frac{m_T}{2T} v^2 \right) , \qquad (9b)$$

and

$$f_\alpha = \beta \, \frac{n_\alpha}{(2\pi T/m_\alpha)^{3/2}} \exp \left(- \frac{m_\alpha}{2T} v^2 \right) + \frac{S_0 \tau_s}{4\pi} \, \frac{1}{v^3+v_c^3} \, U(v_0-v)$$

$$+ \frac{S_0 \tau_s}{4\pi} \, \frac{1}{v_0^3+v_c^3} \exp \{ - \frac{m_\alpha}{2T} (v^2 - v_0^2) \} \, U(v-v_0) . \qquad (9c)$$

Here, β is the bulk fraction of the alpha distribution;

$$\beta = 1 - \frac{S_0 \tau_s}{3 n_\alpha} \ln \frac{v_0^3+v_c^3}{v_c^3}$$

$$- \frac{S_0 \tau_s}{n_\alpha} \, \frac{1}{v_0^3+v_c^3} \, \frac{T}{m_\alpha} \left[v_0 + \sqrt{\frac{\pi T}{2 m_\alpha}} \exp \left(\frac{m_\alpha v_0^2}{2T} \right) \{ 1 - \Phi \left(\sqrt{\frac{m_\alpha}{2T}} v_0 \right) \} \right]$$

$$\simeq 1 - \frac{S_0 \tau_s}{3 n_\alpha} \ln \frac{v_0^3+v_c^3}{v_c^3} - \frac{S_0 \tau_s}{n_\alpha} \, \frac{1}{v_0^3+v_c^3} \, \frac{T}{m_\alpha} \left(v_0 + \frac{T}{m_\alpha} \frac{1}{v_0} \right) , \qquad (10)$$

T the common temperature of bulk ions, τ_s and v_c are the slowing-down time and the critical speed of the alpha particle [11], U and Φ are the step function and the error function, respectively. The first term on the r.h.s. of Eq.(9c) denotes the bulk component of the alpha particles; a group of alpha particles with a Maxwellian distribution and a temperature equal to that of the plasma ions [15]. The second term of f_α is a so-called slowing-down distribution. The last contribution to f_α is due to the spread of the distribution beyond the birth speed by Coulomb collisions, where the electron temperature, T_e, is taken to be the same as T. We set $T=T_e$ hereafter.

The deposited RF power density for the Maxwellian distribution is given by

$$P_{RF,i}^{M} \propto 2\, m_i\, n_i\, \frac{1}{\omega}\, \frac{z_i^2 e^2}{m_i^2}\, |E_+|^2 \sum_{n=0}^{\infty} \frac{(-1)^n}{n!} \left(\frac{k_\perp}{2\omega_{ci}} \sqrt{\frac{2T}{m_i}} \right)^{2n} \times \left[\left(\frac{k_\perp}{2\omega_{ci}} \sqrt{\frac{2T}{m_i}} \right)^{2(N-1)} \frac{N+n}{(N+n-1)!} \frac{\Gamma(2(N-1)+2n+1)}{\Gamma(2(N-1)+n+1)} + \frac{|E_-|^2}{|E_+|^2} \left(\frac{k_\perp}{2\omega_{ci}} \sqrt{\frac{2T}{m_i}} \right)^{2(N+1)} \frac{N+n+2}{(N+n+1)!} \frac{\Gamma(2(N+1)+2n+1)}{\Gamma(2(N+1)+n+1)} \right], \tag{11}$$

where use has been made of the relation,

$$J_l^2\left(\frac{k_\perp v_\perp}{\omega_{ci}}\right) = \sum_{n=0}^{\infty} \frac{(-1)^n}{n!} \left(\frac{k_\perp v_\perp}{2\omega_{ci}}\right)^{2(l+n)} \frac{1}{\{\Gamma(l+n+1)\}^2} \frac{\Gamma(2l+2n+1)}{\Gamma(2l+n+1)}, \tag{12}$$

and Γ is the gamma function. For small $k_\perp \rho_i \equiv k_\perp \sqrt{T/m_i}/\omega_{ci}$ (ρ_i; the Larmor radius of the i-species ion at the thermal speed), (11) reduces to

$$P_{RF,i}^{M} \propto 2\, m_i\, n_i\, \frac{1}{\omega}\, \frac{z_i^2 e^2}{m_i^2}\, |E_+|^2\, \frac{N}{(N-1)!} \left(\frac{k_\perp}{2\omega_{ci}} \sqrt{\frac{2T}{m_i}} \right)^{2(N-1)}. \tag{13}$$

The RF power density absorbed by the alpha particles, $P_{RF,\alpha}$, is obtained from the numerical integration of Eq.(8) with Eq.(9c).

3. ICRF ABSORPTION BY ALPHAS

3.1 Linear absorption

Let us investigate the linear absorption by alphas for three cases of frequencies, $\omega = 2\omega_{cD} = 3\omega_{cT} = 2\omega_{c\alpha}$ (N=2), $\omega = 3\omega_{cD} = 3\omega_{c\alpha}$ (N=3), and $\omega = 4\omega_{cD} = 6\omega_{cT} = 4\omega_{c\alpha}$ (N=4). To clarify the effect of energetic alpha particles and that of bulk alphas, two cases of $\beta = 0$ and $\beta \neq 0$ are studied separately.

(i) β=0 case: Figures 1 and 2 show the dependence of R_α on the electron temperature, $T_e(=T)$, and on ω_{pe}/ω_{ce}, respectively, for β=0, where $n_e=n_D+n_T$ is assumed for simplicity. The values of $|E_-|^2/|E_+|^2$ are ~6.1 for N=2, ~3.2 for N=3, and ~2.3 for N=4 in (a), while $|E_-|$ is set zero in (b). The ratio, ω_{pe}/ω_{ce}, is chosen as 0.5 in Fig.1 and the electron temperature, T_e, is taken to be 20 keV in Fig.2. The T_e dependence of R_α in Fig.1 can be easily understood by considering the following: The ratio of the alpha particle density for the slowing-down distribution to the electron density increases with T; $n_\alpha/n_e \simeq (S_0\tau_s/3n_e)\ln\{(v_0^3+v_c^3)/v_c^3\}$, while the deposited power density for deuterons is proportional to T^{N-1}, as is shown by (13). The value of R_α increases with N, and decreases with ω_{pe}/ω_{ce}. The value of R_α in Fig.2(b) ($|E_-|$=0) is slightly smaller for small ω_{pe}/ω_{ce} and appreciably smaller for large ω_{pe}/ω_{ce} than that in Fig.2(a) ($|E_-| \neq 0$). The cold plasma dispersion relation is followed by the relation, $k_\perp\rho_i \propto \omega_{pe}/\omega_{ce}$. Therefore, the rates of linear absorption by the Maxwellian deuterons and tritons decrease with decreasing ω_{pe}/ω_{ce}, and the contribution of the high energy alpha tail to ICRF absorption becomes notable, in which the $|E_+|^2$ contribution to $P_{RF,i}$ is dominant. On the contrary, the $|E_-|^2$ contribution becomes important for large ω_{pe}/ω_{ce} (low magnetic field or high density).

In the limit of $\omega_{pe}/\omega_{ce} \to 0$, by using Eqs.(8), (9c) with β=0, and (12) we can get

$$P_{RF,\alpha} \propto m_\alpha S_0\tau_s \frac{1}{\omega} \frac{z_\alpha^2 e^2}{m_\alpha^2} |E_+|^2 \left(\frac{k_\perp}{2\omega_{c\alpha}}\right)^{2(N-1)} \frac{2^{2N}N^2}{(2N)!} \int_0^{v_0} dv \frac{v^{2N}}{v^3+v_c^3}, \qquad (14)$$

where the contribution of the distribution in the range, $v \geq v_0$, to $P_{RF,\alpha}$ is neglected. The deposited power density for deuterons, $P_{RF,D}$, is calculated from Expression (13), and that for tritons, $P_{RF,T}$, is negligible. Then, the

following expression of R_α for $\omega_{pe}/\omega_{ce}\to 0$ is obtained;

$$R_\alpha \simeq \frac{P_{RF,\alpha}}{P_{RF,\alpha}+P_{RF,D}} \simeq \frac{1}{1+\left(\frac{T}{E_\alpha}\right)^{N-1}\frac{(2N)!}{(N-2)!}\frac{1}{N\,2^{N-1}}\frac{1}{n_e\tau_s\langle\sigma v\rangle}}\ , \tag{15}$$

where use has been made of the approximation,

$$\int_0^{v_0} dv\ \frac{v^{2N}}{v^3+v_c^3} \simeq \frac{v_0^{2(N-1)}}{2(N-1)}\ . \tag{16}$$

Expression (15) is applicable for $N \ll E_\alpha/T$. For T=20 keV, (15) gives the following values; R_α~0.54(N=2), 0.95(N=3), and 1.0(N=4). They are consistent with the extrapolated values of R_α shown in Fig.2 at ω_{pe}/ω_{ce}=0. Thus we can see the appreciable absorption of the higher harmonic ($N\geqq 3$) cyclotron waves by the alpha particles.

(ii) $\beta\fallingdotseq 0$ case: Figure 3 shows the dependence of the rates of linear absorption by alphas (α), deuterons (D), and tritons (T) on the alpha concentration, n_α/n_e, for (a) $\omega=2\omega_{cD}$, (b) $\omega=3\omega_{cD}$, and (c) $\omega=4\omega_{cD}$ in the case of $\beta>0$. The parameters are as follows; T=20 keV and ω_{pe}/ω_{ce}=0.824 (e.g., the electron density of $n_e=2\times10^{14}$ cm^{-3} and the toroidal magnetic field of B_T=5.5 T). The values of $|E_-|^2/|E_+|^2$ are (a) 6.1 - 8.7, (b) 3.2 - 3.9, and (c) 2.3 - 2.7. In the figure, β is also plotted by the dashed line. The rate, R_α, increases with n_α/n_e, although the dependence of R_α on n_α/n_e is weak in the range, e.g., $n_\alpha/n_e < 0.1$ for T = 20 keV, where the contribution of high energy alpha particles with the slowing-down distribution is dominant in $P_{RF,\alpha}$ compared with that of bulk alphas. Figure 4 shows R_i as a function of n_α/n_e for ω_{pe}/ω_{ce}=0.206. Other parameters are the same as those in Fig.3. When R_α for the alpha slowing-down distribution is nearly unity, as in the case of smaller ω_{pe}/ω_{ce} and larger $N(\geq 3)$ (Fig.4 (b) and (c)), the increase of n_α/n_e leads to the slight decrease of R_α in the range where the contribution of the high energy alphas is dominant. This is because the high energy alpha tail population diminishes owing to the decrease of the fuel ion densities and hence of the fusion reaction rate, $S_0 = n_D n_T\langle\sigma v\rangle = (0.5-n_\alpha/n_e)^2\, n_e^2\langle\sigma v\rangle$. As n_α/n_e becomes much larger and the contribution of the bulk alphas overcomes the high energy alpha contribution, R_α approaches

to $R_\alpha^M \equiv P_{RF,\alpha}^M/(P_{RF,D}^M+P_{RF,T}^M+P_{RF,\alpha}^M)$, which indicates the rate of RF power density absorbed by the bulk alphas. For small $k_\perp\rho_i$, the dependence of R_α^M on n_α/n_e is easily obtained by using Expression (13);

$$R_\alpha^M \simeq \frac{n_\alpha/n_e}{2^{N-3} - (2^{N-2} - 1)\, n_\alpha/n_e} . \tag{17}$$

3.2 Fusion reactivity enhancement

In this subsection, effects of ICRF wave absorption by alpha particles on the fusion reactivity enhancement due to the wave induced ion tail are investigated by taking into account of the deformation of the distribution functions due to the ICRF waves. The distribution is evaluated by averaging Eq.(1) over ξ and truncating the Legendre expansion of f_i at zero order. Such a one-dimensional semi-analytical calculation is in good agreement with the two-dimensional numerical one at least in the low RF power density [10-12]. Figure 5 shows R_i as a function of $\hat{P}_{RF}$ ($\equiv P_{RF}/(n_eT_e/2\tau_s)$) for (a) $\omega=2\omega_{cD}$, (b) $\omega=3\omega_{cD}$, and (c) $\omega=4\omega_{cD}$. The plasma parameters are T=20 keV, $n_e=2\times10^{14}$cm^{-3}, n_α/n_e=1/10, and B_T=5.5 T. The values of $|E_-|^2/|E_+|^2$ are (a) 6.6, (b) 3.3, and (c) 2.4. The value of R_α decreases with increasing $\hat{P}_{RF}$, which is accompanied by the deformation of the distributions (Fig.6). This is because the deuteron tail induced by the ICRF wave further couples with the wave [11]. Figure 6 shows the distribution functions, $\hat{f}_i \equiv f_i/n_i\times(T/m_i)^{3/2}$, of alphas ($\alpha$), deuterons (D), and tritons (T) in the logarithmic scale versus the particle energy normalized by T for $\omega=2\omega_{cD}$ at $\hat{P}_{RF}\sim10$. The value of $|E_-|^2/|E_+|^2$ is 6.6 in (a), while it is set zero in (b). It is seen that the low energy alpha particles constitute a bulk component. ICRF enhancement of the high energy tail in the finite $|E_-|^2/|E_+|^2$ case is more appreciable than that in the $|E_-|^2/|E_+|^2$=0 case. This effect of the finite $|E_-|^2/|E_+|^2$ leads to the vain acceleration of fuel ions from the reactivity enhancement point of view, as is shown later. Mainly discussed in what follows is the aspects of the fusion reactivity enhancement by the ion tail formation for various harmonic numbers in the presence of the alpha particles. Figure 7 shows the fusion reactivity, $\langle\sigma v\rangle$, normalized by that with Maxwellian deuteron and triton distributions (at P_{RF}=0) as a function of $\hat{P}_{RF}$ for n_α/n_e=0 (dashed lines) and 1/10 (solid lines). The RF frequency is chosen as (a) $\omega=2\omega_{cD}$, (b) $\omega=3\omega_{cD}$, (c) $\omega=4\omega_{cD}$, and (d) $\omega=2\omega_{cT}$. Two cases of $|E_-|^2/|E_+|^2\simeq0$ and

$|E_-|^2/|E_+|^2=0$ are indicated. The plasma parameters are T=20 keV, $n_e=2\times10^{14}cm^{-3}$, and B_T=5.5 T. Fusion reactivity enhancement by the ion tail formation in high temperature plasmas is generally ineffective, since high energy particles accessible to the energy region near the peak point, E_*(~130 keV), of the D-T fusion cross section are sufficiently contained in the Maxwellian distribution [11]. Namely, ions affected by the ICRF waves tend to be accelerated above E_* vainly from the reactivity enhancement point of view. This feature is furthered by the effect of the finite $|E_-|^2/|E_+|^2$ in higher $\hat{P}_{RF}$, which results in saturation of $\langle\sigma v\rangle$. The maximum attainable values of $\langle\sigma v\rangle$ for $\omega=N\omega_{cD}$ (a-c) decrease with increasing N, and $\langle\sigma v\rangle$ for larger N saturates in the lower $\hat{P}_{RF}$ value; in the case of $|E_-|^2/|E_+|^2\fallingdotseq0$, these $\hat{P}_{RF}$ values are ~10 for N=2, ~5 for N=3, and ~2.5 for N=4. This is not only because the higher energy ions are accelerated vainly owing to the higher harmonic resonance, but also because the rate of ICRF absorption by the alpha particles increases with N. The fusion reactivity enhancement for $\omega=2\omega_{cT}$ (d) becomes ineffective with increasing $\hat{P}_{RF}$ owing to the large $|E_-|^2/|E_+|^2$ value of 20 - 30, although the reactivity without the $|E_-|^2/|E_+|^2$ effect for $\omega=2\omega_{cT}$ is enhanced as further as that for $\omega=2\omega_{cD}$ (a). The enhanced reactivity is changed a little by the presence of alpha particles for n_α/n_e less than 1/10. The alpha concentration lowers the fuel ion densities, which leads to the large deformation of the distribution functions of the fuel ions at the low RF power density. Therefore, the effective enhancement of $\langle\sigma v\rangle$ in the presence of alpha particles is found for $\omega = 2\omega_{cT}$ (d) without alpha particle resonance. The large deformation in the larger $\hat{P}_{RF}$ region, however, brings the vain acceleration, and $\langle\sigma v\rangle$ for n_α/n_e = 1/10 (solid line) becomes smaller than that for n_α/n_e = 0 (dashed line). For the cases of (a), (b), and (c), $\langle\sigma v\rangle$ becomes small in the presence of alpha particles. This is because the effect of the RF power absorption by high energy alpha particles exceeds the effect of the enlarged deformation mentioned above.

When P_{RF} is small, an offset-linear relation of the fusion power density, P_F, proportional to $\langle\sigma v\rangle$ against P_{RF} is obtained;

$$P_F = Q^* P_{RF} + P_{F0} \ , \tag{18}$$

where P_{F0} is the fusion power density for the Maxwellian deuteron and triton distributions, and the energy of 17.6 MeV is assumed to be released per one

fusion reaction. The gain factor, Q^*, defined by Eq.(18) denotes the figure of merit of enhancement of the fusion power density at the low RF power density. Figure 8 shows the maximum value of Q^* versus ω/ω_{cD} for n_α/n_e = 0 (diamonds), 1/100 (squares), and 1/10 (triangles). It is noted that $\omega = 2\omega_{cT}$ corresponds to $\omega = 4/3\omega_{cD}$. Two cases of B_T = 5.5 T (open symbols) and 11 T (black symbols) are illustrated. Other plasma parameters are T = 20 keV and $n_e = 2\times10^{14}$ cm^{-3}, and $|E_-|^2/|E_+|^2 \fallingdotseq 0$. In the case without absorption by alphas (n_α/n_e = 0 ; diamonds), higher values of Q^*_{max} are achieved by higher harmonic heating, although the windows of P_{RF} for increasing the reaction rates are not large as compared with the window of the case, $\omega = 2\omega_{cD}$ (Fig.7). On the other hand, Q^*_{max} is deteriorated because of the wave absorption by the alpha particles with the finite concentration (n_α/n_e = 1/100 ; squares and 1/10 ; triangles): The values of Q^*_{max} for $\omega = 3\omega_{cD}$ and $4\omega_{cD}$ are almost the same as or smaller than those for $\omega = 2\omega_{cD}$ and $2\omega_{cT}$ in the case of B_T = 5.5 T. In high B_T of 11 T, further decrease of Q^*_{max} can be seen for higher harmonic heating.

4. CONCLUSIONS

We have investigated ICRF wave absorption by alpha particles and the fusion reactivity enhancement due to the ICRF induced ion tail. The rate of linear absorption by the alpha slowing-down distribution increases with the cyclotron harmonic number, and decreases with ω_{pe}/ω_{ce}. The rate in the finite $|E_-|^2/|E_+|^2$ case becomes large as compared with that in the $|E_-|^2/|E_+|^2$=0 case, which is pronounced for large ω_{pe}/ω_{ce}. Increase of the thermal alphas leads to the formation of the alpha bulk component. This results in the further increase of the rate of absorption by alphas, unless that for the slowing-down distribution is nearly unity. ICRF enhancement of the high energy ion tail in the finite $|E_-|^2/|E_+|^2$ case is more appreciable than that in the $|E_-|^2/|E_+|^2$=0 case. This leads to the vain acceleration of the fuel ions from the reactivity enhancement point of view. The figure of merit of enhancement of the fusion power density is deteriorated because of the wave absorption by the alpha particles, especially for higher harmonic heating in the high magnetic field. Second harmonic ICRF heating is comparatively applicable to the enhancement of the fusion power density even in the pre-

fusion reaction. The gain factor, Q^*, defined by Eq.(18) denotes the figure of merit of enhancement of the fusion power density at the low RF power density. Figure 8 shows the maximum value of Q^* versus ω/ω_{cD} for n_α/n_e = 0 (diamonds), 1/100 (squares), and 1/10 (triangles). It is noted that $\omega = 2\omega_{cT}$ corresponds to $\omega = 4/3\omega_{cD}$. Two cases of B_T = 5.5 T (open symbols) and 11 T (black symbols) are illustrated. Other plasma parameters are T = 20 keV and $n_e = 2\times10^{14}$ cm^{-3}, and $|E_-|^2/|E_+|^2 \fallingdotseq 0$. In the case without absorption by alphas (n_α/n_e = 0 ; diamonds), higher values of Q^*_{max} are achieved by higher harmonic heating, although the windows of P_{RF} for increasing the reaction rates are not large as compared with the window of the case, $\omega = 2\omega_{cD}$ (Fig.7). On the other hand, Q^*_{max} is deteriorated because of the wave absorption by the alpha particles with the finite concentration (n_α/n_e = 1/100 ; squares and 1/10 ; triangles): The values of Q^*_{max} for $\omega = 3\omega_{cD}$ and $4\omega_{cD}$ are almost the same as or smaller than those for $\omega = 2\omega_{cD}$ and $2\omega_{cT}$ in the case of B_T = 5.5 T. In high B_T of 11 T, further decrease of Q^*_{max} can be seen for higher harmonic heating.

4. CONCLUSIONS

We have investigated ICRF wave absorption by alpha particles and the fusion reactivity enhancement due to the ICRF induced ion tail. The rate of linear absorption by the alpha slowing-down distribution increases with the cyclotron harmonic number, and decreases with ω_{pe}/ω_{ce}. The rate in the finite $|E_-|^2/|E_+|^2$ case becomes large as compared with that in the $|E_-|^2/|E_+|^2$=0 case, which is pronounced for large ω_{pe}/ω_{ce}. Increase of the thermal alphas leads to the formation of the alpha bulk component. This results in the further increase of the rate of absorption by alphas, unless that for the slowing-down distribution is nearly unity. ICRF enhancement of the high energy ion tail in the finite $|E_-|^2/|E_+|^2$ case is more appreciable than that in the $|E_-|^2/|E_+|^2$=0 case. This leads to the vain acceleration of the fuel ions from the reactivity enhancement point of view. The figure of merit of enhancement of the fusion power density is deteriorated because of the wave absorption by the alpha particles, especially for higher harmonic heating in the high magnetic field. Second harmonic ICRF heating is comparatively applicable to the enhancement of the fusion power density even in the pre-

sence of the alpha particles, which may lead to the burn control of nearly ignited plasmas. Higher harmonic ICRF waves can be appropriate for heating of the alpha particles.

The present work is based on the local analysis. Global analyses taking into account, for example, electron Landau damping of the ICRF waves and alpha cyclotron damping in the outer region are left to future studies.

ACKNOWLEDGEMENTS

The authors would like to thank Dr. Y. Kishimoto and Dr. T. Takeda for valuable discussions and continuous encouragements.

sence of the alpha particles, which may lead to the burn control of nearly ignited plasmas. Higher harmonic ICRF waves can be appropriate for heating of the alpha particles.

The present work is based on the local analysis. Global analyses taking into account, for example, electron Landau damping of the ICRF waves and alpha cyclotron damping in the outer region are left to future studies.

ACKNOWLEDGEMENTS

The authors would like to thank Dr. Y. Kishimoto and Dr. T. Takeda for valuable discussions and continuous encouragements.

REFERENCES

[1] WONG, K.L., ONO, M., Nucl. Fusion 24 (1984) 615.
[2] BONOLI, P.T., PORKOLAB, M., Nucl. Fusion 27 (1987) 1341.
[3] STIX, T.H., Nucl. Fusion 15 (1975) 737.
[4] KESNER, J., Nucl. Fusion 18 (1978) 781.
[5] BLACKFIELD, D.T., SCHARER, J.E.,
Nucl. Fusion 22 (1982) 255.
[6] PEKKARI, L.O., ANDERSON, D., HAMNEN, H., LISAK, M.,
Nucl. Fusion 23 (1983) 781.
[7] SCHARER, J., JACQUINOT, J., LALLIA, P., SAND, F.,
Nucl. Fusion 25 (1985) 435.
[8] KRAPCHEV, V.B., Nucl. Fusion 25 (1985) 455.
[9] HARVEY, R.W., McCOY, M.G., KERBEL, G.D., CHIU, S.C.,
Nucl. Fusion 26 (1986) 43.
[10] ANDERSON, D., CORE, W., ERIKSSON, L.G., HAMNEN, H.,
HELLSTEN, T., LISAK, M., Nucl. Fusion 27 (1987) 911.
[11] YAMAGIWA, M., TAKIZUKA, T., KISHIMOTO, Y.,
Nucl. Fusion 27 (1987) 1773.
[12] YAMAGIWA, M., TAKIZUKA, T., KIMURA, H., AZUMI, M.,
to be published in Plasma Phys. Controll. Fusion.
[13] RAM, A., BERS, A., Nucl. Fusion 24 (1984) 679.
[14] STIX, T.H., The Theory of Plasma Waves, McGraw-Hill,
New York (1962).
[15] KOLESNICHENKO, Ya.I., FURSA, A.D.,
Fiz. Plazmy 1 (1975) 806; Sov. J. Plasma Phys. 1 (1975) 442.

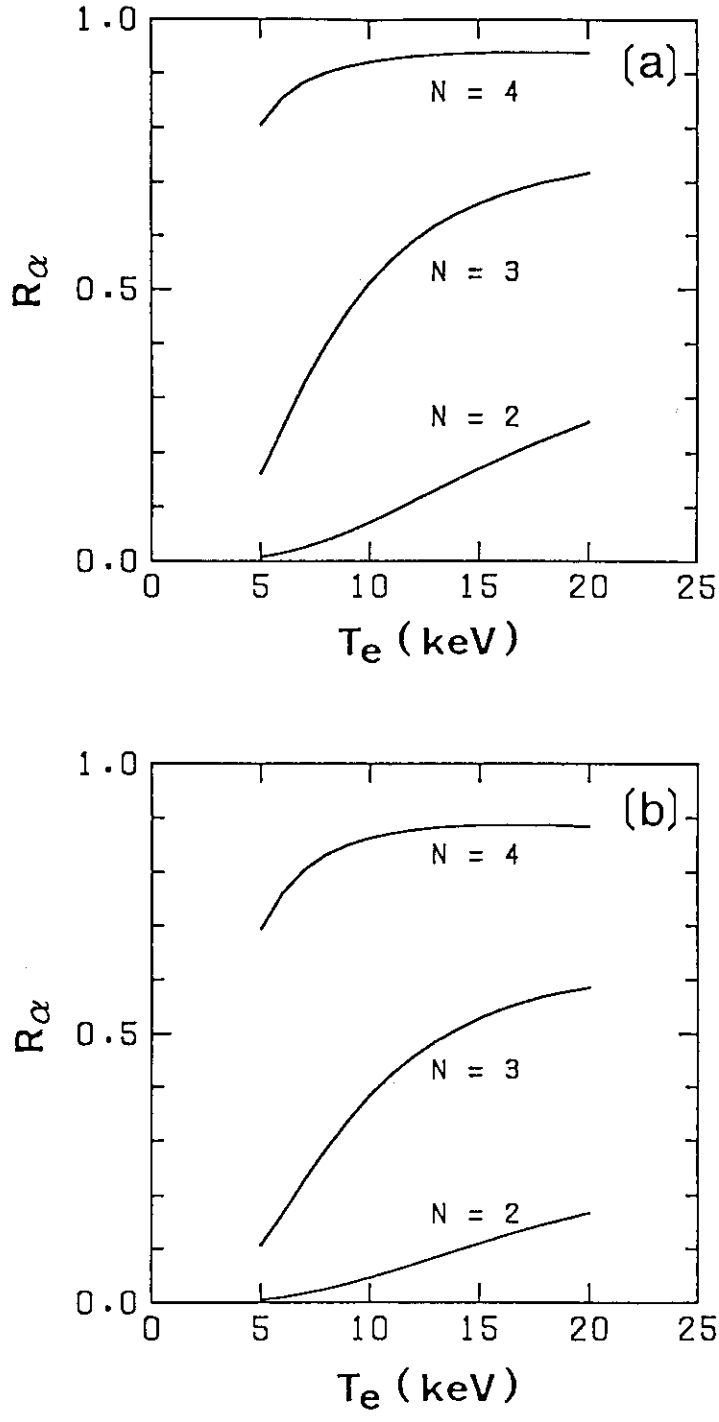

Fig. 1 Rate of linear absorption by slowing-down distribution of alpha particles, R_α, versus T_e in keV for $N=\omega/\omega_{cD}$ = 2, 3, and 4. Ion temperature is equal to electron temperature. The ratio, ω_{pe}/ω_{ce}, is 0.5. Values of $|E_-|^2/|E_+|^2$ are ~6.1 for N=2, ~3.2 for N=3, and ~2.3 for N=4 in (a), while $|E_-|$ is set zero in (b).

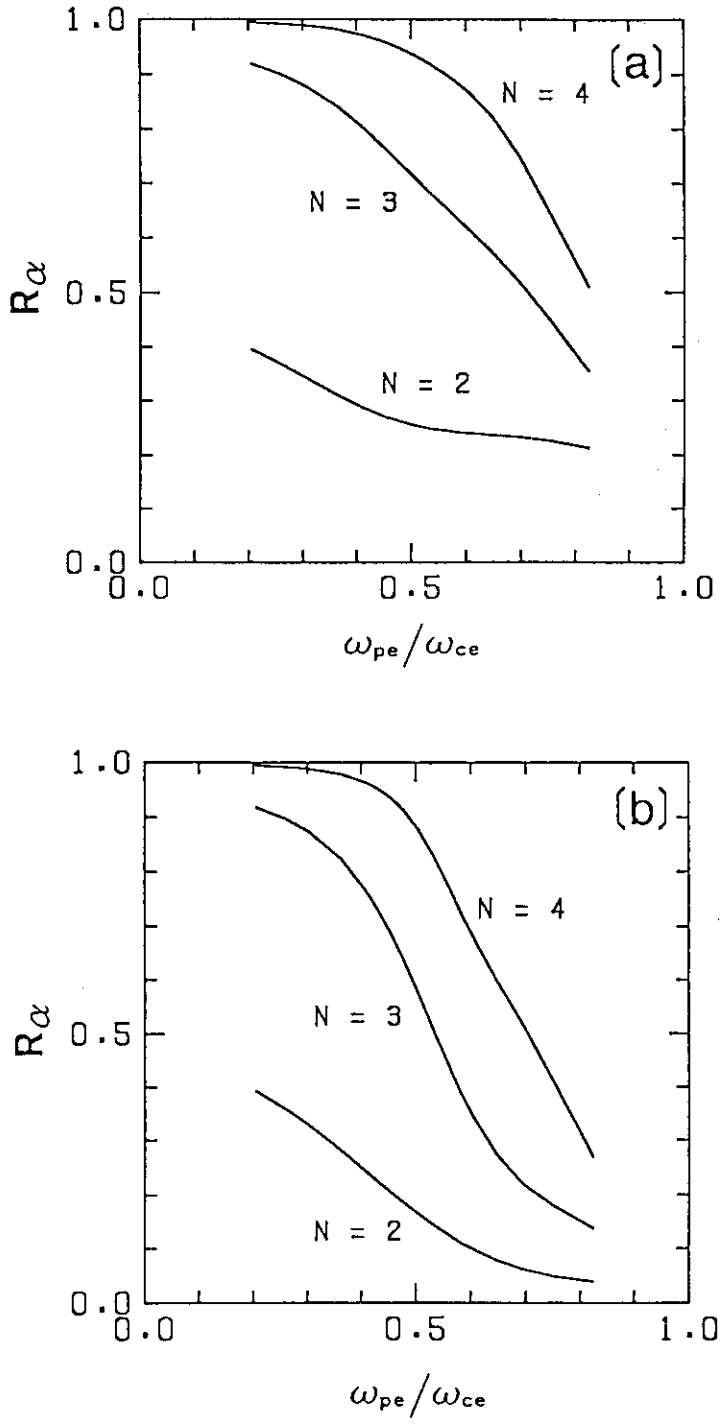

Fig. 2 Rate of linear absorption by slowing-down distribution of alpha particles, R_α, versus ω_{pe}/ω_{ce} for $N=\omega/\omega_{cD}$ = 2, 3, and 4. The electron temperature, T_e, is 20 keV. Values of $|E_-|^2/|E_+|^2$ are ~6.1 for N=2, ~3.2 for N=3, and ~2.3 for N=4 in (a), while $|E_-|$ is set zero in (b).

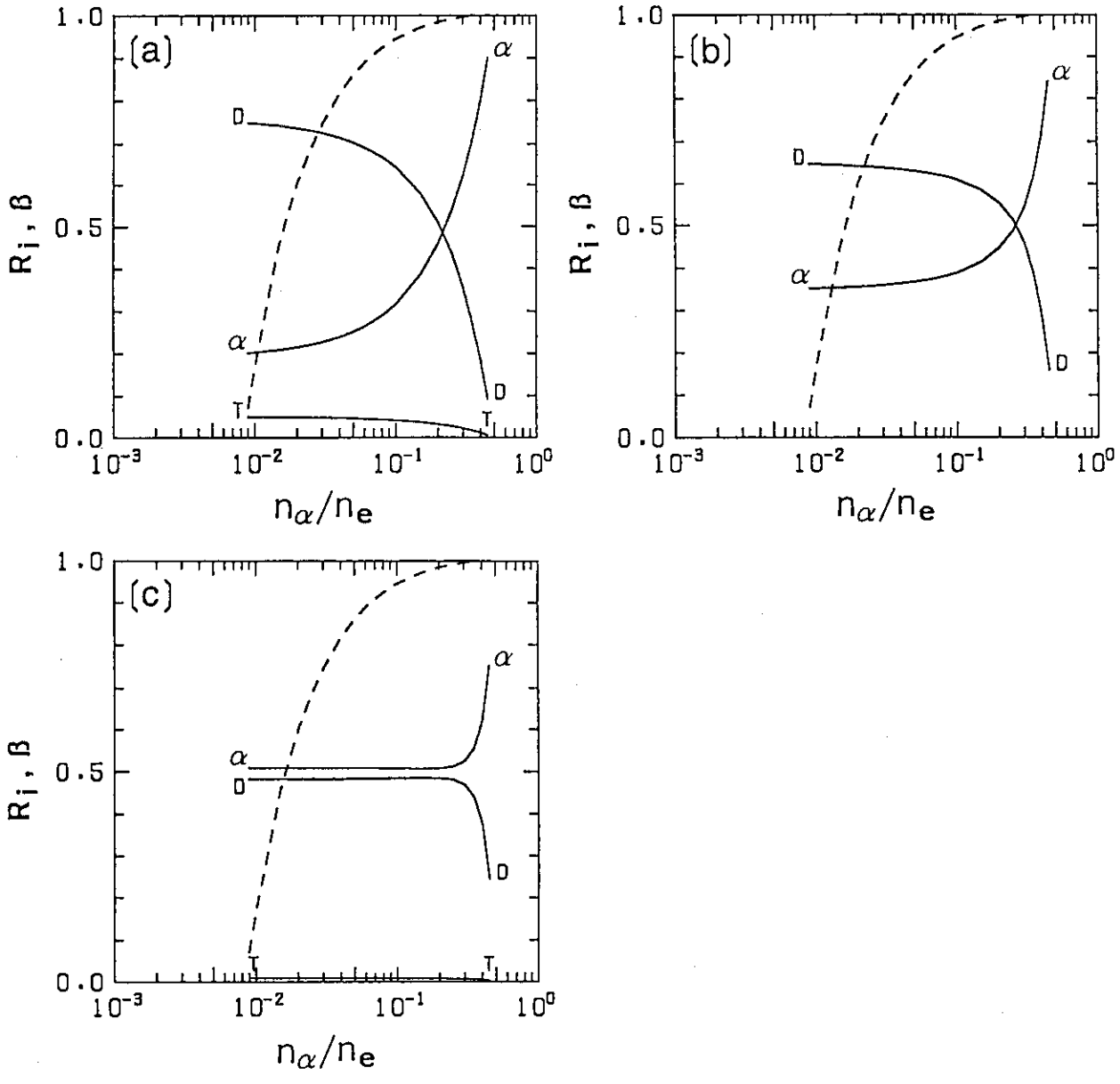

Fig. 3 Rates of linear absorption by alphas (α), deuterons (D), and tritons (T) versus n_α/n_e for (a) $\omega=2\omega_{cD}$, (b) $\omega=3\omega_{cD}$, and (c) $\omega=4\omega_{cD}$. Bulk fraction of alpha distribution, β, is also plotted by dashed line. Plasma parameters are T =20 keV and ω_{pe}/ω_{ce}=0.824. Values of $|E_-|^2/|E_+|^2$ are (a) 6.1 - 8.7, (b) 3.2 - 3.9, and (c) 2.3 - 2.7.

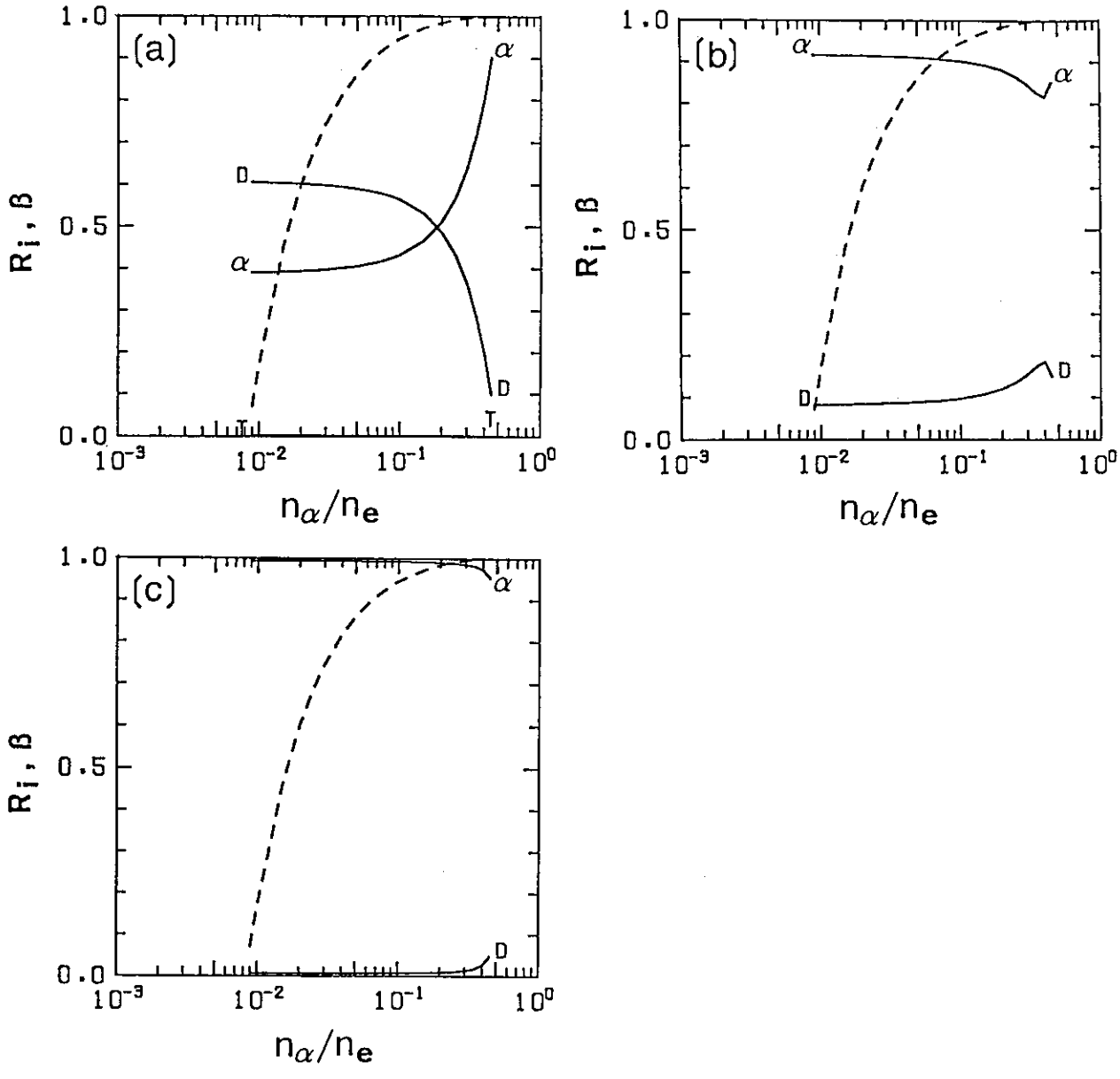

Fig. 4 Rates of linear absorption by alphas (α), deuterons (D), and tritons (T) versus n_α/n_e for (a) $\omega=2\omega_{cD}$, (b) $\omega=3\omega_{cD}$, and (c) $\omega=4\omega_{cD}$. Bulk fraction of alpha distribution, β, is also plotted by dashed line. Plasma parameters are T =20 keV and ω_{pe}/ω_{ce}=0.206. Values of $|E_-|^2/|E_+|^2$ are (a) 6.1 - 8.7, (b) 3.2 - 3.9, and (c) 2.3 - 2.7.

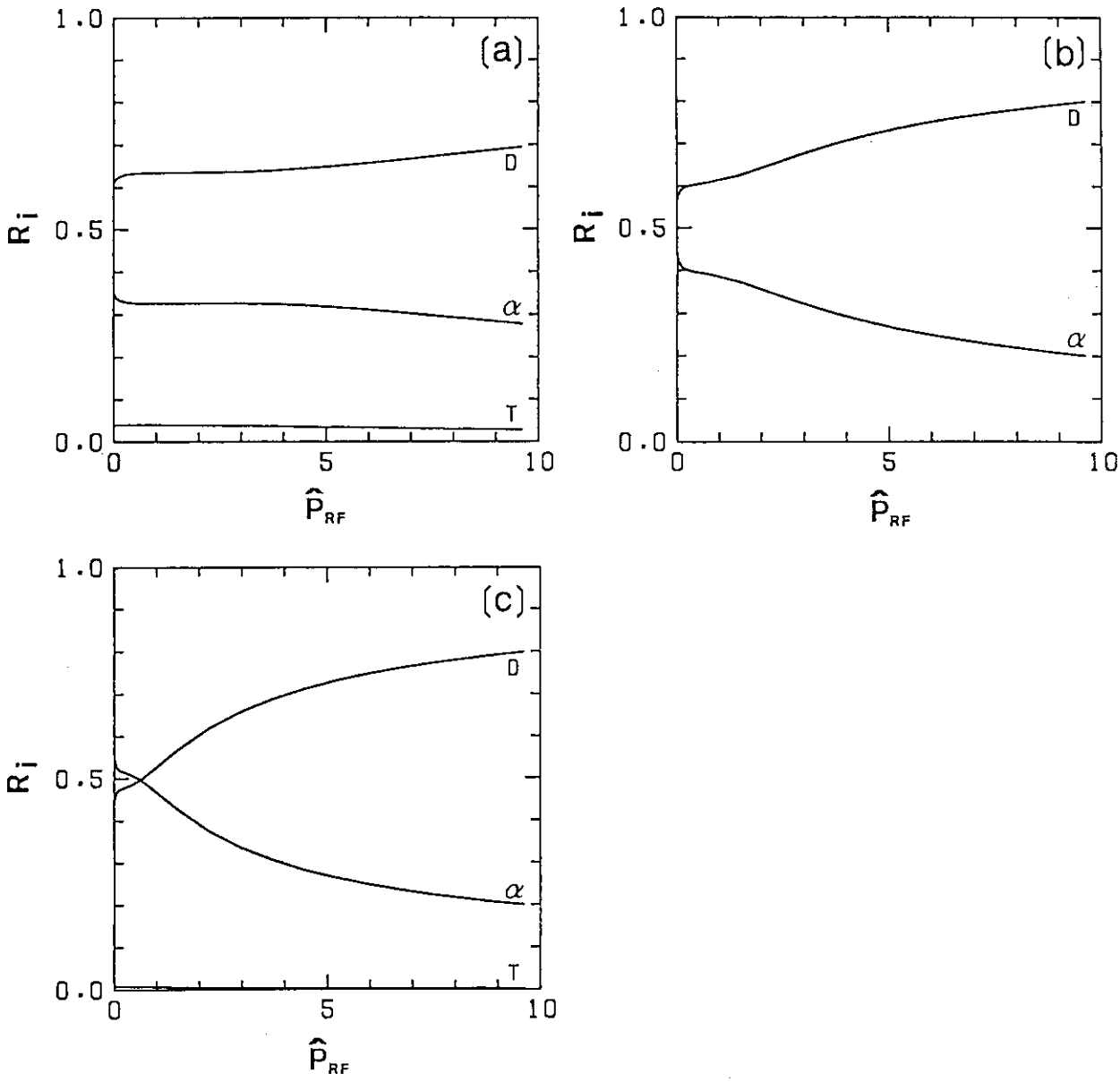

Fig. 5 Rates of ICRF absorption by alphas (α), deuterons (D), and tritons (T) as a function of $\hat{P}_{RF}$ for (a) $\omega=2\omega_{cD}$, (b) $\omega=3\omega_{cD}$, and (c) $\omega=4\omega_{cD}$. Plasma parameters are T =20 keV, $n_e=2\times10^{14}cm^{-3}$, $n_\alpha/n_e=1/10$, and B_T=5.5 T. Values of $|E_-|^2/|E_+|^2$ are (a) 6.6, (b) 3.3, and (c) 2.4.

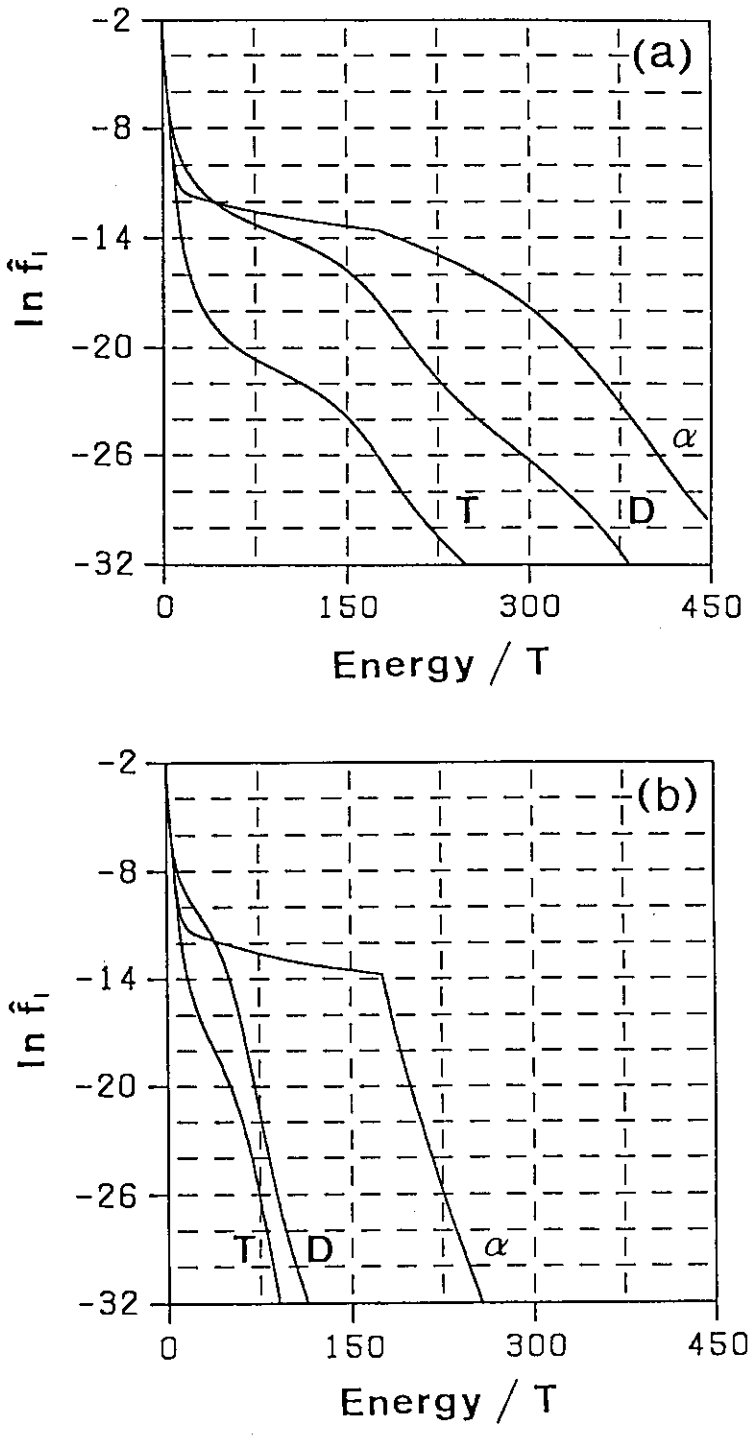

Fig. 6 Distribution functions of alphas (α), deuterons (D), and tritons (T) versus particle energy for $\omega=2\omega_{cD}$ at $P_{RF}\sim10$. Value of $|E_-|^2/|E_+|^2$ is 6.6 in (a), while it is set zero in (b). Plasma parameters are T =20 keV, $n_e=2\times10^{14}cm^{-3}$, $n_\alpha/n_e=1/10$, and B_T=5.5 T.

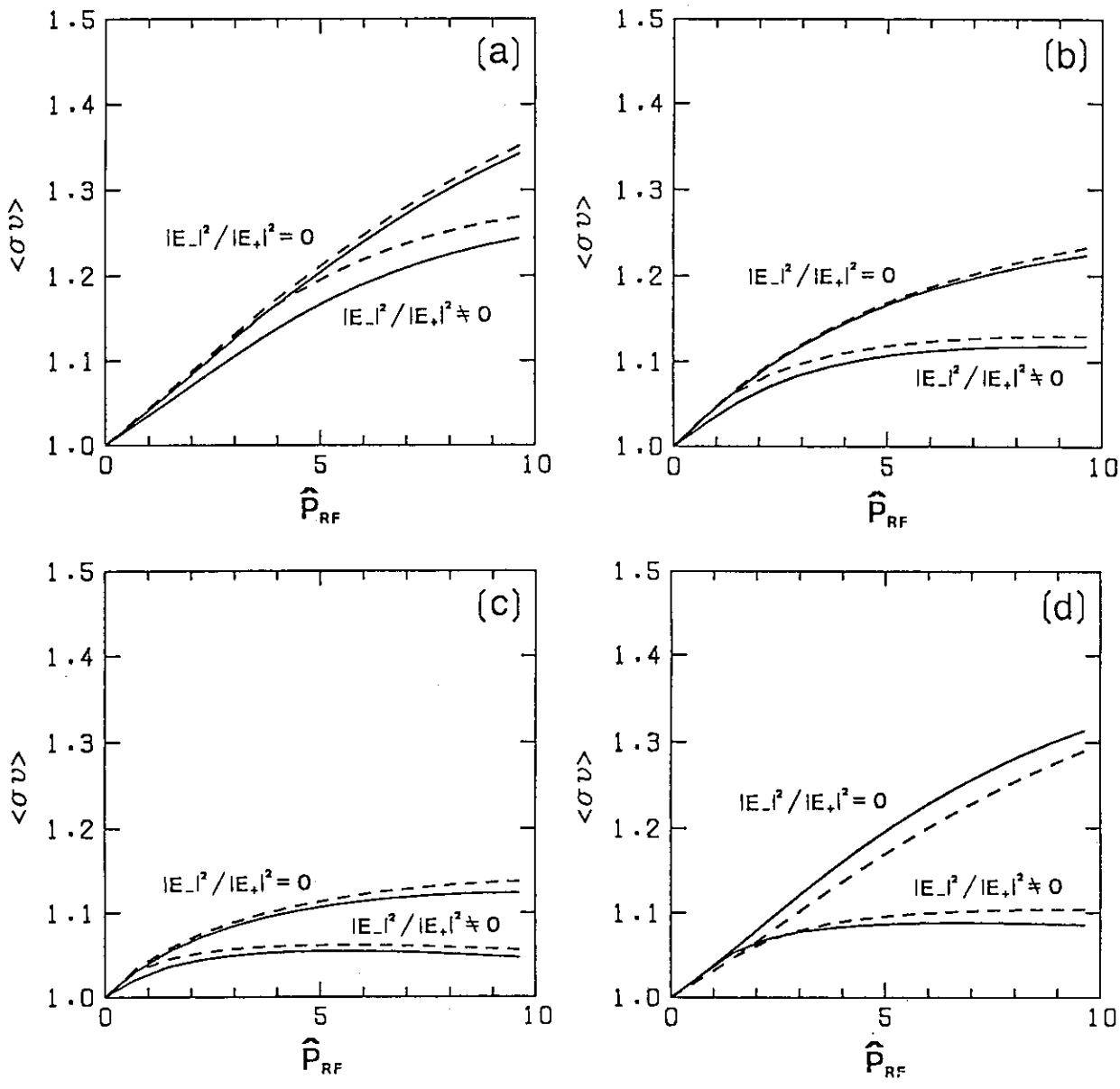

Fig. 7 Fusion reactivity normalized by that with Maxwellian deuteron and triton distributions, $\langle\sigma v\rangle$, as a function of $\hat{P}_{RF}$ for n_α/n_e=0 (dashed lines) and 1/10 (solid lines). RF frequency is chosen as (a) $\omega=2\omega_{cD}$, (b) $\omega=3\omega_{cD}$, (c) $\omega=4\omega_{cD}$, and (d) $\omega=2\omega_{cT}$. Plasma parameters are T =20 keV, $n_e=2\times10^{14}$cm^{-3}, and B_T=5.5 T. For $|E_-|\neq0$, $\langle\sigma v\rangle$ is smaller than that for $|E_-|=0$.

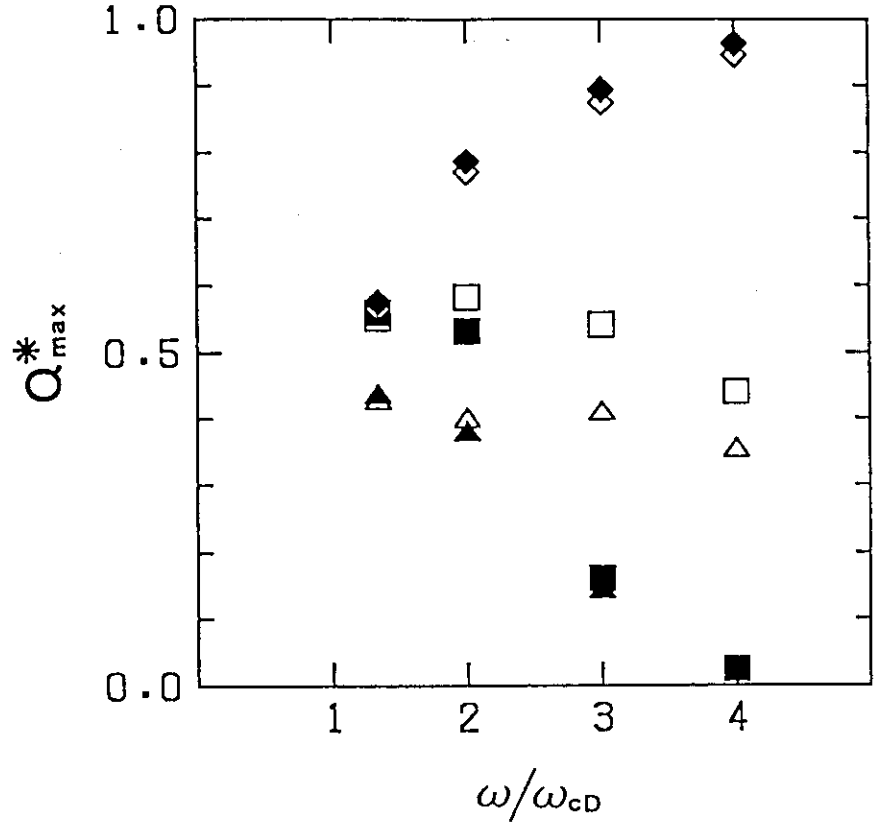

Fig. 8 Maximum value of Q^* versus ω/ω_{cD} for n_α/n_e=0 (diamonds), 1/100 (squares), and 1/10 (triangles). Two cases of B_T=5.5 T and 11 T are illustrated by open symbols and black symbols, respectively. Other plasma parameters are T =20 keV and n_e=2×10^{14}cm^{-3}, and $|E_-|^2/|E_+|^2$≒0.